JOURNAL GEOLOGICAL SOCIETY OF INDIA
Vol.95, February 2020, pp.152-158

Potential Use of Airborne Hyperspectral AVIRIS-NG Data for Mapping Proterozoic Metasediments in Banswara, India

Komal Rani[1]*, Arindam Guha[1], K. Vinod Kumar[1], Bimal Kumar Bhattacharya[2], B. Pradeep[3]

[1]Geosciences Group, National Remote Sensing Centre (ISRO), Hyderabad – 500 037, India

[2]Biological and Planetary Sciences Group, Earth Ocean Atmosphere Planetary Sciences and Applications Area, Space Applications Centre (ISRO), Ahmedabad - 380 015

[3]Andhra University, Visakhapatnam - 530 003

***E-mail:** pasrichakomal@gmail.com*

ABSTRACT

Airborne Visible InfraRed Imaging Spectrometer – Next Generation (AVIRIS-NG) data with high spectral and spatial resolutions are used for mapping metasediments in parts of Banswara district, Rajasthan, India. The AVIRIS–NG image spectra of major metasedimentary rocks were compared with their respective laboratory spectra to identify few diagnostic spectral features or absorption features of the rocks. These spectral features were translated from laboratory to image and consistently present in the image spectra of these rocks across the area. After ensuring the persistency of absorption features from sample to image pixels, three AVIRIS – NG based spectral indices is proposed to delineate calcareous (dolomite), siliceous (quartzite) and argillaceous (phyllite) metasedimentary rocks. The index image composite was compared with the reference lithological map of Geological Survey of India and also was validated in the field. The study demonstrates the efficiency of AVIRIS – NG data for mapping metasedimentary units from the Aravalli Supergroup that are known to host strata bound mineral deposits.

INTRODUCTION

Earth and Planetary surfaces have been well studied using spaceborne imaging spectrometer with different spatial and spectral resolutions in last three decades (van der Meer et al., 2012). Imaging spectroscopy uses the diagnostic absorption features from the reflectance spectra of rocks and minerals for target detection (Goetz et al., 1985; Clark,1999, Clark et al., 2003). Imaging spectroscopy is capable to detect these absorption features irrespective of the distance of the sensor from the target (Clark, 1999).

Airborne hyperspectral data with different spectral and spatial resolution have been used for mineral mapping or large scale geological mapping (Farrand, 1997; Kratt, 2010; Bedini, 2011). The Airborne Visible InfraRed Imaging Spectrometer (AVIRIS) was one of the most popular and widely used airborne hyperspectral sensors; which have 224 bands and spectral resolution of 10 nm. Hyperspectral data acquired from airborne platform has the combined benefit of higher spectral and spatial resolution as against the established multispectral image data. The efficiency of AVIRIS sensor has been demonstrated in a number of studies. Kruse et al. (1993) used a knowledge based expert mineral system and linear spectral unmixing methods to identify the spatial distribution of spectrally distinct minerals occurring both as primary rock forming minerals, secondary alteration and weathering products using AVIRIS data. Crowley (1993) attempted to map evaporite minerals in the Death Valley in California, although these minerals are aspectral (there is no absorption feature) within the spectral bandwidth of AVIRIS data. AVIRIS data were also used for mapping minerals associated with the hydrothermal alterations, playas, geobotanically stressed zones indicative of hydrocarbon seepages(e.g. presence of hydrocarbon beneath the subsurface causes the disturbance in the growth of vegetation at the surface) (Kruse et al., 1993; Baugh et al., 1998 Boardman and Kruse, 1994; Boardman et al., 1995; Kruse et al., 2003). In another study, AVIRIS data was used as a proxy to map the concentration of minerals (e.g. buddingtonite) having diagnostic absorption features in hydrothermally-altered volcanic rocks in the southern Cedar Mountains, Esmeralda County (Baugh et al., 1998). In this study, authors demonstrated a simple quantitative relation between absorption depth in the mineral spectra at 2.12 μm and the concentration of mineral phase. In the effort to analyse the utility of different mapping algorithms in target detection, potentials of spectral angle mapper and Tricorder algorithm were tested for mapping kaolinite group of minerals and ferric oxides based on processing of AVIRIS data (Crosta et al., 1998). It has been noted that results obtained using AVIRIS and Hyperion (hyperspectral datasets) data give comparable results in mineral mapping(Kruse et al., 2003). These are illustrative examples of the potential of AVIRIS data operated from airborne platform in delineating geological targets.

It is always a challenge to delineate metasedimentary rocks in tropical/ sub-tropical weathering conditions based on their spectral contrast using remote sensing data. Presence of thick soil and alluvial cover, patchy or scanty surface exposures of the rocks and similar constituent minerals (dominated by quartz and feldspar) are some of the inherent obstacles in using spectral signatures for mapping such rocks in India. It is therefore not surprising that very few studies on these lines have been attempted using hyperspectral data (Bhattacharya et al., 2019; Govil et al., 2018; Jain et al., 2018).

The AVIRIS – New Generation (AVIRIS – NG) sensor has a superior spectral resolution (5 nm) than the AVIRIS sensor (10 nm) and hence is expected to give enhanced capabilities for mineral and lithological mapping.AVIRIS – NG data were acquired for the selected sites under the joint collaboration of National Aeronautics and Space Administration (NASA) and Indian Space Research Organization (NASA, 2018). Under this collaboration, AVIRIS – NG data were acquired for different geological sites spread over the entire stretch of India. In the present study, AVIRIS – NG data were collected from approximate height of 4 km. This has resulted acquisition of AVIRIS – NG data with approximately 4 meter spatial resolution with 5 nm spectral resolution (Kruse et al., 2002; Thorpe et al., 2016). In this study, attempt has been made to assess the potential of AVIRIS – NG data for mapping patchy exposures of dolomite and associated metasedimentary rocks of Proterozoic age of Aravalli Supergroup. They are known to host strata bound or lithology controlled deposit like Pb – Zn in Zawar area, Phosphate in Jhamarkotra area and Gold deposits in Bhukia area (Deb and Bhattacharya, 1980; Choudhuri et al., 1986; Mukherjee, 1988; Gupta et al., 2010; Mukherjee and Venkatesh, 2017; Rani et al., 2019). Therefore, accurate mapping of these metasedimentary rocks of the study area is important. In this

DOI: 10.1007/s12594-020-1404-5 | 0016-7622/2020-95-2-152/$ 1.00

study, we have tested proposed AVIRIS – NG based indices using the absorption features in their spectra to delineate different metasediments and also tested their utility in delineating these rocks.

STUDY AREA AND GEOLOGY

The study area is located at fifty kilometer north – east of Banswara, Rajasthan which is well connected with Udaipur and Ratlam. In the study area, metasedimentary rocks of the Aravalli Super Group are exposed (Fig. 1). Major rock units of the study area are dolomite, quartzite and phyllite (Fig. 2). The area is deeply weathered; scattered agriculture activities are located on quartzite and phyllite whereas dolomite rich zones constitute pediment surfaces of rock exposures. Dolomite and quartzite also forms denudational, structural ridges at selective places. Geological trend of the rocks is along NW – SE and these metasediments were deposited as platformal deposit in the Paleoproterozoic Sea (Banerjee, 1971; Roy and Paliwal, 1981). Stratigraphically, these rocks belong to lower Aravalli Super Group and it is part of Udaipur Group (made up with phyllite, quartzite, meta-conglomerate and dolomite etc, The lithological units occur in this part of Banswara region are presumed to be the continuation of central Udaipur sector (Roy and Jhakhar, 2002). Dry Deciduous Forests (Teak Mixed) has been found in Banswara districts and forest cover is dominant land cover at the north western part of the study area.

MATERIALS AND METHODS

Materials

AVIRIS – NG data: AVIRIS – NG is a hyperspectral sensor of

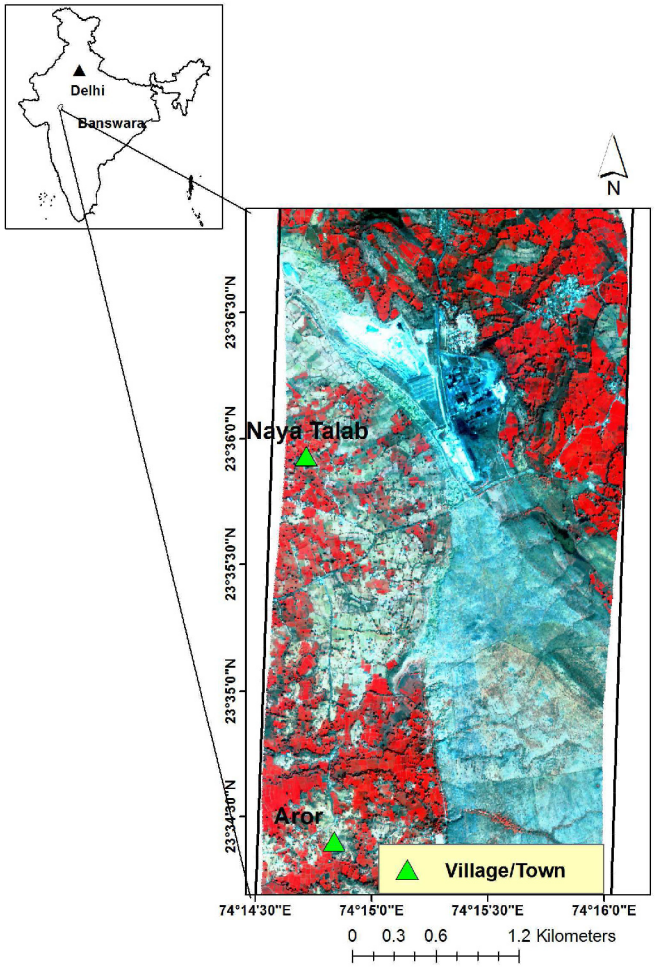

Fig.1 Location map of study area. Study area boundary is draped over AVIRIS-NG false colour composite (FCC) image using band 98=Red, band 56=Green, band 36=Blue colour.

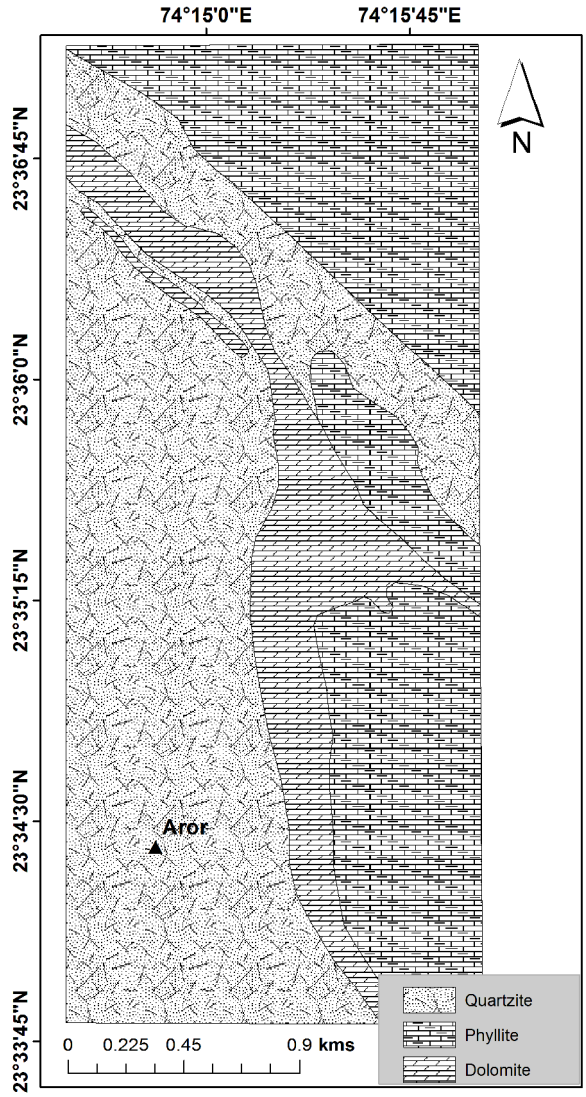

Fig.2. Lithological map of the study area (GSI, 2000).

NASA – Jet Propulsion Laboratory (JPL). This sensor collects the spectral data within the wavelength range from 380 nm to 2510 nm with 5 nm spectral resolution. AVIRIS NG data are captured with 600 pixels along the swath. AVIRIS – NG data for this study were collected using aircraft with flying height of 4 km and yielding a spatial resolution of approximately 4 m. We have used "at sensor radiance" data product of AVIRIS – NG sensor for this study. Broad outline of AVIRIS – NG sensor is given in Table 1. Methodology flow chart has been given in Fig. 3.

Ancillary data: Geological maps (prepared by the Geological Survey of India in 1:50000 scale) for the study area is used for analyzing the spectral maps delineating different rock types. The boundaries of litho units were updated using standard false colour composite of AVIRIS-NG data(using spectral bands at 850 nm, 650 nm and 560 nm in Red-Green-Blue colour display). Spectral profiles of three

Table 1. AVIRIS – NG band specification

Date of Acquisition	Feb 3, 2016
Spectroradiometer	VNIR and SWIR
No. of Bands	1 to 425
Wavelength Ranges	380 nm – 2510 nm
Spectral Resolution	5 nm ± 0.5 nm
Spatial Resolution	Approx. 4 m
Radiometric Resolution	14 bits

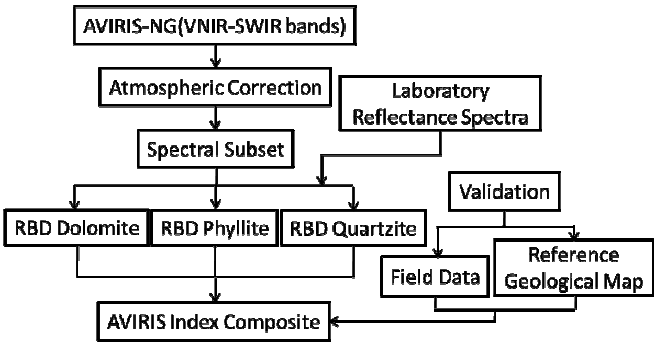

Fig.3. Flow chart of methodology

lithounits are analysed using Fieldspec 3© spectroradiometer (ASD, 2015). The spectrometer is capable of collecting spectral data within the spectral range of 350-2500 nm with the spectral resolution of 1.4 nm between 350 - 1050 nm; and 2.0 nm between 1000 - 2500 nm (ASD, 2015). Spectral profiles collected using spectrometer were resampled to the spectral resolution 5 nm to match spectral resolution of AVIRIS-NG sensor. These spectral profiles are used as reference for identifying suitable spectral bands of AVIRIS – NG data to delineate different rock types.

Methods

AVIRIS Pre – processing and spectral data collection: The AVIRIS – NG Level 1B data ("georectified at sensor radiance") were processed for mapping the major rocks of the study area. In this regard, we calibrated the "at sensor georectified radiance data" to "scaled-reflectance" based on MODTRAN – 4 (MODerate resolution atmospheric TRANsmission) atmospheric calibration model implemented using FLAASH (Fast line-of-sight atmospheric analysis of spectral hypercube) algorithm (Kaufman et al., 1997). This atmospheric correction algorithm has been widely used in applications of remotely sensed hyperspectral data to correct for the effects of atmospheric propagation on spectral radiance acquired by space-borne systems. It helps in converting acquired radiance values to reflectance values, which can then be used for target detection (Cooley et al., 2002; Felde et al., 2003). After calibrating the radiance data to reflectance, we removed band striping, other systematic noises and also calculated data dimensionality using minimum noise fraction (MNF) image. MNF image is derived by calculating principal components from the noise whitened data of AVIRIS – NG sensor (Green et al., 1988). MNF bands were sequentially arranged with increasing effect of noise and poorer spectral variance as the MNF order increases. The MNF bands with high signal to noise ratio (SNR) and spectral content were selected for inverse transform operation to transfer the spectral information from MNF data space to the original dimension of spectral bands. Spectral quality of the data was evaluated by comparing the image spectra of deciduous tree, dolomite with their AVIRIS – NG resampled laboratory spectra. This helps to ascertain the performance of FLAASH calibration. We masked vegetation using normalized difference vegetation index (NDVI) image using 860 nm band and 650 nm band from AVIRIS-NG data as vegetation and crop dominated areas would not be suitable for spectral enhancement of rock types.

Fieldspec3© spectrometer was used to collect reflectance spectra of rocks (ASD, 2015). Reflectance spectra were collected within the spectral domain of 350 – 2500 nm, following standard procedures (Price, 1995; Milton et al., 2009; Guha et al., 2012). Radiance of the representative samples of different litho-units were normalized using radiances from completely spectacular Lambertian surfaces to derive reflectance spectra. During field survey, we collected the rock samples to carry out spectral analysis of samples under laboratory condition; these samples were collected from the exposed surface of structural, denudational hills and pediments. Rock samples (for each rock type) collected in the study represent the local variations due to weathering and associated impurities. Two to three rock samples of each rock types were cut into slabs of 4"x5" dimensions and spectra were collected for few spots of a sample of each rock type., Samples were irradiated with halogen lamp (for simulating solar irradiance) for recording laboratory spectra. Reflected radiance from samples were collected and subsequently normalized with the reflected radiance of white Lambertian plate to derive the reflectance at each wavelength. The spectra of rock samples were constructed by plotting the reflectance of the sample with reference to wavelength range of spectroradiometer. Spectra collected from five to six sample spots of samples of each rock type were used to derive mean reflectance spectrum of representative sample of each rock type. Subsequently, spectra of all the samples of same rock were averaged to derive reflectance spectrum of each rock. These spectra were used for deriving the index image after resampling them, using the spectral bands of AVIRIS – NG sensor; which represent laboratory spectra well.

AVIRIS – NG data processing : AVIRIS – NG resampled laboratory spectra of rocks were compared with each other to understand the separability of the diagnostic absorption features of different rocks in wavelength domain of AVIRIS sensor (Fig.6). Image spectra were collected from those pixels; which were regarded as representative surface exposures of each rock type inclusive of variability resulted due to weathering and impurity. Further, AVIRIS – NG image spectra of different rocks were compared with their respective laboratory spectra to understand consistency of diagnostic spectral features /absorption features from laboratory to image (Fig.6) (Matthew et al. 2000). We identified diagnostic spectral features or absorption features of each rock with their respective shoulders (i.e. the edge of the absorption feature defining localised reflectance maxima) and absorption minimas (i.e. wavelength of maximum absorption) in their image spectra and compared them with the corresponding features in laboratory spectra. These absorptions features were imprinted on their rock spectra due their spectrally sensitive constituent minerals. The representative rock spectrum of dolomite was characterised with absorption minima at 2.33 micrometer, quartzite had absorption at 2.2 micrometer. Phyllite had two absorption features with absorption minima at 2.16 micrometer and 2.3 micrometer. Using the matches in the image and laboratory spectra, we derived Relative Band Depth (RBD) images for each litho-type. Spectral bands of AVIRIS – NG having same or similar wavelength with the wavelength of diagnostic absorption feature of each rock were used to derive RBD image. RBD images were derived using the selected SWIR bands of the AVIRIS – NG as absorption features of litho-units were identified within the SWIR domain (Table 2). Utility of RBD images for enhancing rock types is well known fact in the field of geological remote sensing (Rowan and Mars, 2003; Yamaguchi and Naito, 2003; Gad and Kusky, 2007). Further, RBD image like band ratio image can detect target exposed under different illumination condition (Lillesand et al., 2014). RBD image composites were derived by combining individual RBD image of each rock for delineating metasediments using AVIRIS – NG data in single image product. Geological map of the study area has been taken as the reference to verify the utility of AVIRIS – NG index image for delineating different rocks. In this regard, quantitative validation of AVIRIS – NG image with reference to the geological map of the study area was attempted using the confusion matrix analysis (Story and Congalton, 1986; Combar et al., 2012) for the small portion of the study area. Image enhanced product derived using three RBD image was vectorised for small area for comparison with the updated geological map of the area. Results of Quantitive validation map derived from conjugate

Table 2. Details of AVIRIS – NG derived indices. B1= Calcareous Index; B2= Argillaceous index; B3= Siliceous Index

AVIRIS-NG Bands (central wavelength (μm))	Rock type	Index (Relative Band Depth)	Colour of specific rock in Index composite image
band 373 (2.2397) band 392 (2.3348) band 404 (2.3949)	Dolomite	$B1 = \frac{band\ 373 + band\ 404}{band 392}$	Red and Magenta
band 353 (2.1395) band 366 (2.2046) band 378 (2.2647)	Phyllite	$B3 = \frac{band\ 340 + band\ 366}{band 348}$	Green
band 340 (2.0744) band 348 (2.1144) band 366 (2.2046)	Quartzite	$B2 = \frac{band\ 353 + band\ 378}{band 366}$	Blue

FCC image of three RBD image or FCC images were summarized in the Table 3.

RESULTS AND DISCUSSION

As mentioned in introduction section, the main focus of this work was to analyse the potential of the spectral bands of AVIRIS – NG in delineating major metasediments of Aravalli Super Group (Lower Proterozoic in age) based on derivation of optimum image enhanced products using the continuous and contiguous spectral bands of AVIRIS-NG airborne hyperspectral data. The study area has exposures of different metasedimentary lithounits and also covered with forest and agriculture (Fig.1 and Fig.2). The aim was to derive image enhanced products from "at-sensor-radiance" data of AVIRIS-NG sensor to evaluate the potential of imaging spectroscopy in discriminating different litho- units based on their diagnostic absorption features. With this AVIRIS-NG data were processed systematically after synchronising laboratory reflectance spectra of rocks with their respective AVIRIS-NG image spectra (Fig.3). Image pixels representative of prominent surface exposures of rocks were used for collecting image spectra (Fig, 4.a to c). We analysed the quality of relative reflectance image (AVIRIS-NG); which was derived based on implementation of MODTRAN based calibration on "at-sensor radiance" data (Fig. 4a. and b). We observed that the overall shape of deciduous tree and dolomite spectra-derived from AVIRIS image correspond well with the respective the AVIRIS resampled laboratory-derived spectra of same elements (Fig.5.a, b). This justifies the potential of AVIRIS-NG data in preserving the reflectance spectra of rocks. Checking of calibration quality of the AVIRIS – NG data is important before mapping different geological targets using spectral profiles of targets as reference.

Subsequently, spectral analysis of image and laboratory spectra of rocks was carried out. In this regard, we analysed the spectra of each rocks collected in laboratory and we found few diagnostic absorption features; which were diagnostic to spectral feature of the spectrally conspicuous constituent mineral. Different literature on mineral spectroscopy and mineralogy of the rocks of the study area were proved useful to analyse these absorption feature (Roy and Paliwal, 1981; Shaif et al., 2017; Fatima et al., 2017). For example, dolomite has diagnostic absorption feature at 2.33 micrometer and this feature is contributed by the constituent mineral dolomite. Quartzite has

Table 3. Confusion matrix analysis of accuracy assessment of index image composite with respect to published lithological map

Overall Accuracy = (136163/154475) 88.15%				
Kappa Coefficient = 0.8217				
Class	Dolomite	Quartzite	Phyllite	Total
Dolomite	53182	354	471	54007
Quartzite	2386	44901	7000	54287
Phyllite	1859	6242	38080	46181
Total	57427	51497	45551	154475
Commission and Omission errors (Percent)				
Class	Commission (Percent)		Omission(Percent)	
Dolomite	1.53		7.39	
Quartzite	17.29		12.81	
Phyllite	17.54		16.40	
Producer and User Accuracy				
Class	Prod. Acc. (Percent)		User Acc. (Percent)	
Dolomite	92.61		98.47	
Quartzite	87.19		82.71	
Phyllite	83.60		82.46	

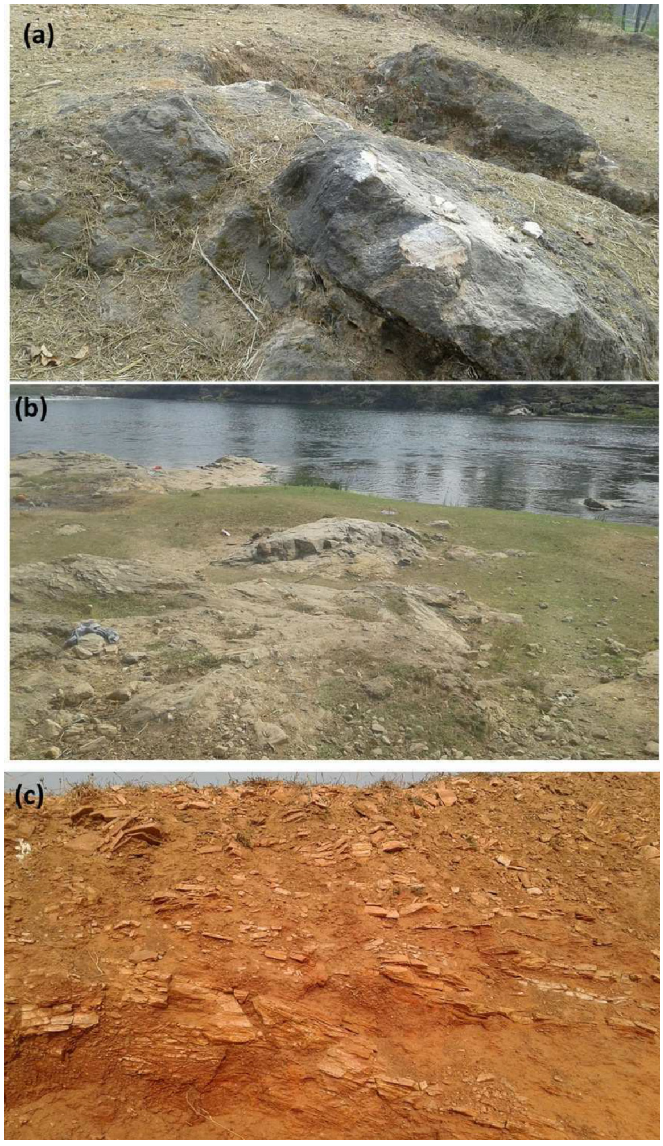

Fig.4. Field photographs of **(a)** dolomite, **(b)** quartzite and **(c)** phyllite at selected locations in the study area.

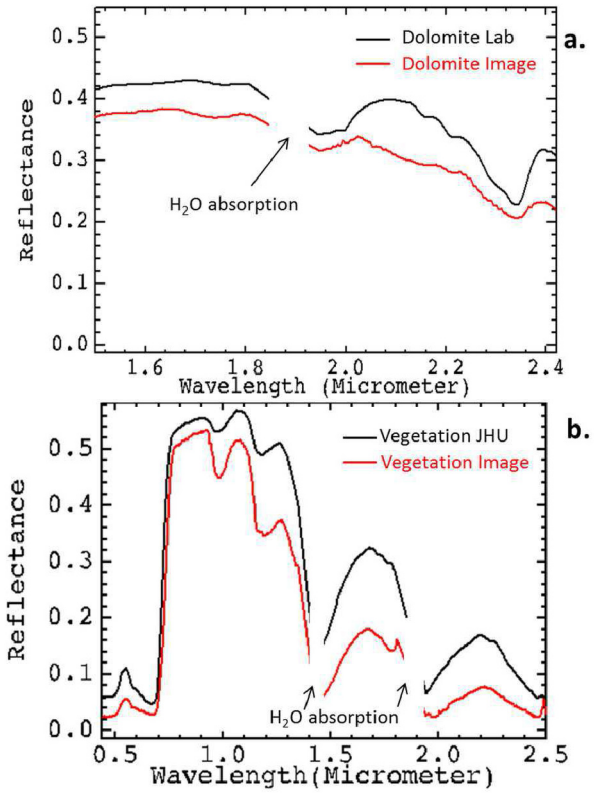

Fig.5. **(a)** Comparison of image spectra of dolomite derived from calibrated AVIRIS data with corresponding laboratory spectra of dolomite **(b)** Comparison of image spectra of vegetation derived from calibrated AVIRIS data with corresponding laboratory spectra of deciduous forest (JHU: John Hopkins University) (Guha et al., 2019).

diagnostic feature at 2.2 micrometer could due to presence of micaceous minerals with with quartz. Phyllite is constituted with kaolinite (around 2.12 micrometer) and chlorite (2.3 micrometer) (Roy and Paliwal, 1981; Shaif et al., 2017; Fatima et al., 2017). The wavelengths of diagnostic absorption features of dolomite, quartzite and phyllite were identified at 2.3 micrometer, 2.2 micrometer and 2.16 micrometer respectively (Fig. 6. a, b and c). We found all of the diagnostic features of rocks were also preserved in their image spectra. Subsequently, we identified appropriate spectral bands of AVIRIS–NG sensor; which could be used to represent the diagnostic absorption feature of each rock. In this regard, we derived indices or RBD images by selecting spectral bands matching with two shoulders and the absorption minima of absorption feature (Fig.7; Table 2). Therefore, RBD image is suitable index image to delineate targets as RBD derived from hyperspectral data can preserve the shape of the diagnostic absorption feature. AVIRIS – NG Hyperspectral sensor is also suitable to derive accurate relative depth images as it can define accurately the wavelength of absorption depth minima and shoulder or edge of absorption feature due its finer bandwidth of spectral bands than the multispectral bands; which generally have larger spectral bandwidth.

RBD image composite images of siliceous (quartzite), carbonate (dolomite) and argillaceous (phyllite) rocks derived from AVIRIS – NG SWIR bands could delineate these rocks in the spatial domain on the AVIRIS data. False colour composite derived using proposed carbonate rock RBD, siliceous rock RBD and argillaceous rock RBD could delineate each rock from the other and the colour composite image of three RBD image brings out combined spectral contrast of three rocks effectively (Fig. 7). In AVIRIS RBD FCC image, quartzite (blue), residuum above quartzite (Magenta) phyllite (yellowish green) and dolomite (pinkish red) were spectrally enhanced based on their colour and the hue variations of the rocks were also found consistent.

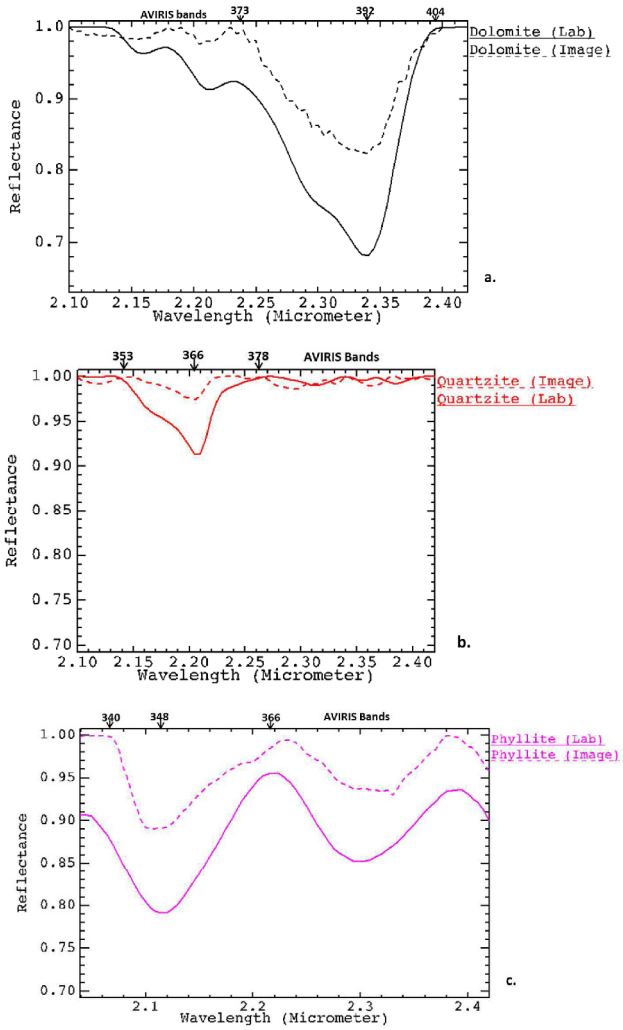

Fig.6. AVIRIS-NG resampled laboratory spectra (solid line) and corresponding image spectra (dashed line) of **(a)** dolomite, **(b)** quartzite and **(c)** phyllite.

The AVIRIS – NG RBD image composite delineating three major rock types were validated quantitatively using the geological map as reference. In this regard, quantitative cross comparison of vectorised version of RBD FCC image and geological map was attempted for specific portion of the area where rock exposures are dominant using confusion matrix analysis. Over all accuracy of the map (compared for only exposure dominated area) of three rocks derived from RBD FCC image was 88.15% with kappa coefficient of 0.82 (Fig.6 and Table 3). This index image product was also validated in the field at selected locations. The producer and user accuracies of the AVIRIS image index composite was lower for phyllite and higher for dolomite and quartzite (Table 3). Producer accuracy was estimated by deriving probability that a value in a given class was classified accurately. User accuracy was used as the probability estimate that a value predicted to be in a certain class really is that class. Errors of commission were used to estimate the fraction of values that were predicted to be in particular class but actually were not classified as the part of that class and Errors of omission represent the fraction of values that belong to a specific class but were classified in a different class (Congalton, 1991). Lower mapping accuracy of phyllite is attributed to intra-pixel spectral mixing resulted due to smaller and highly weathered exposures of foliated and crumbled surface exposures of phyllite. Intra-pixel mixing of phyllite with weathered residuum and land cover developed above this rock modify the image spectra of phyllite in few places and this resulted lower mapping accuracy (Table 3).

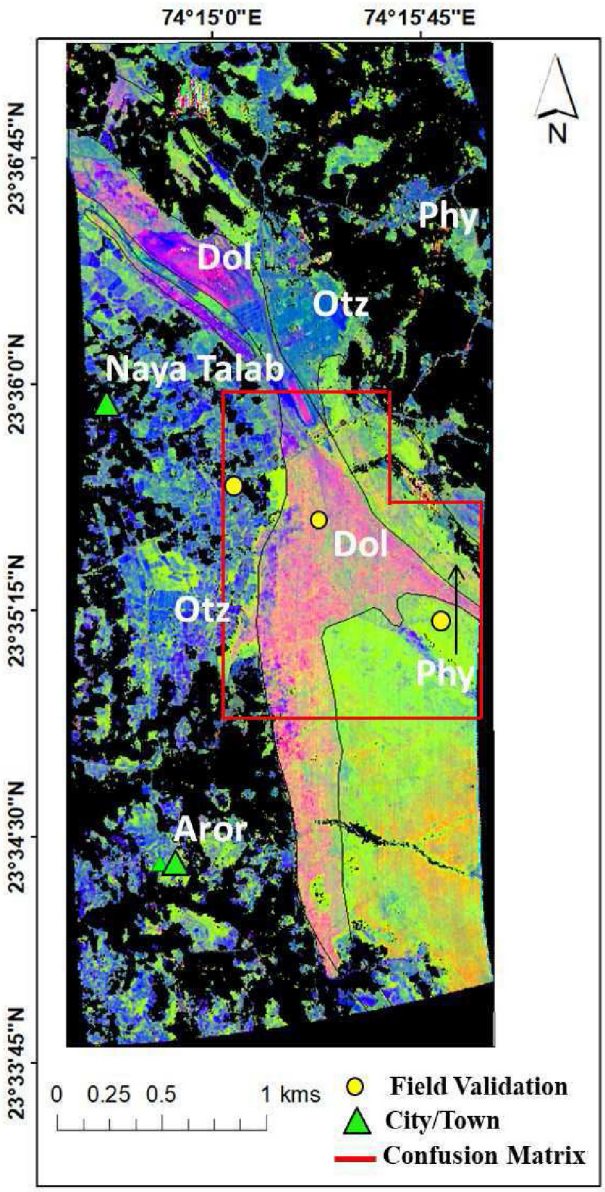

Fig.7. AVIRIS RBD based colour composite derived using three RBD image . Red= Calcareous RBD, Green= Argillaceous RBD and Blue=Siliceous RBD, In this image, Dol: dolomite, Phy: Phyllite, Qtz: Quartzite. Outline of the area analysed for accuracy assessment using confusion matrix analysis.

CONCLUSIONS

High spectral resolution of AVIRIS-NG sensor provides the scope to accurately identify the shoulders (wavelength of observed high reflection points at either side of the absorption features) and absorption minima (wavelength of lowest reflectance observed within the absorption feature) of a spectral feature or absorption feature.Accurate estimation of wavelength of shoulders and absorption minima is essential for targeting rocks and minerals based derivation of RBD images. Continuous and contiguous bands of AVIRIS-NG are suitable to derive RBD-indices for those rocks and minerals; which have very closely spaced diagnostic absorption feature in terms of wavelength. This is true for metasedimentary rocks similar to the rocks analysed in the present study. This is otherwise not possible using broadband spectral data of multispectral sensor.

Based on the results of the study, following are the conclusions derived:

- AVIRIS-NG sensor can enhance spectral separability of metasediments; which have closely spaced spectral feature/ absorption features in wavelength domain of the sensor and the RBD image proposed using AVIRIS – NG data could delineate different metasediments efficiently.
- Further, purity of spectral signatures of geological targets such as metasedimentary rocks is maintained in the AVIRIS-NG image due to high spatial resolution of the AVIRIS-NG data. High Signal to noise ratio (SNR) of the airborne spectral data acquired by AVIRIS-NG sensor also would be suitable to highlight spectral contrast of rocks efficiently.
- Methodology proposed here can be used for deriving spectral indices/RBD images for any rock types using AVIRIS-NG data. Spectral indices derived using airborne hyperspectral bands provide scope to accurately characterize the shoulder and absorption minima of diagnostic absorption /spectral features. This is otherwise difficult using broad spectral bands of multispectral sensor; which have larger bandwidth and hardly can record the wavelength and reflectance of "shoulder" and "absorption minima" of absorption /spectral feature.

References

ASD (2015) Analytical Spectrum Device Inc.,https://www.asdi.com/products-and-services/fieldspec-spectroradiometers (visited on 15-03-2015).

Bedini, E. (2011) Mineral mapping in the Kap Simpson complex, central East Greenland, using HyMap and ASTER remote sensing data. Adv. in Space Res., v.47(1), pp.60-73.

Banerjee, D.M. (1971).Precambrian stromatolitic phosphorites of Udaipur, Rajasthan, India. Geol. Soc. Amer. Bull., v.82(8), pp.2319-2330.

Baugh, W.M., Kruse, F.A. and Atkinson Jr, W.W. (1998) Quantitative geochemical mapping of ammonium minerals in the southern Cedar Mountains, Nevada, using the Airborne Visible/Infrared Imaging Spectrometer (AVIRIS). Remote Sensing Environ., v.65(3), pp.292-308.

Bhattacharya, S., Kumar, H., Guha, A., Dagar, A.K., Pathak, S., Rani, K., Mondal, S., Kumar, K.V., Farrand, W., Chatterjee, S. and Ravi, S. (2019) Potential of airborne hyperspectral data for geo-exploration over parts of different geological/metallogenic provinces in India based on AVIRIS-NG observations. Curr. Sci., v.116(7), pp.1143-1156.

Boardman, J.W., Kruse, F.A. and Green, R.O. (1995) Mapping target signatures via partial unmixing of AVIRIS data: *in* Summaries, Fifth JPL Airborne Earth Science Workshop, JPL Publication 95-1, v.1, pp. 23-26.

Boardman J.W. and Kruse, F.A. (1994) Automated spectral analysis: A geologic example using AVIRIS data, north Grapevine Mountains, Nevada: in Proceedings, Tenth Thematic Conference on Geologic Remote Sensing, Environmental Research Institute of Michigan, Ann Arbor, MI, pp. 1407 – 1418.

Clark, R.N. (1999) Spectroscopy of rocks and minerals, and principles of spectroscopy. Manual of remote sensing, v.3(3-58), pp.2-2.

Clark, R.N., Swayze, G.A., Livo, K.E., Kokaly, R.F., Sutley, S.J., Dalton, J.B., McDougal, R.R. and Gent, C.A. (2003) Imaging spectroscopy: Earth and planetary remote sensing with the USGS Tetracorder and expert systems. Jour. Geophys. Res.: Planets, 108(E12).

Congalton, R.G. (1991) A review of assessing the accuracy of classifications of remotely sensed data. Remote Sensing Environ., v.37(1), pp.35-46.

Choudhuri, R., Roy, A.B., Cook, P.J. and Shergold, J.H. (1986) Proterozoic and Cambrian phosphorites deposits: Jhamarkotra, Rajasthan, India. Proterozoic and Cambrian Phosphorite. Cambridge Univ. Press, Cambridge, pp.209-210.

Comber, A., Fisher, P., Brunsdon, C. and Khmag, A. (2012) Spatial analysis of remote sensing image classification accuracy. Remote Sensing Environ., v.127, pp.237-246.

Cooley, T., Anderson, G.P., Felde, G.W., Hoke, M.L., Ratkowski, A.J., Chetwynd, J.H., Gardner, J.A., Adler-Golden, S.M., Matthew, M.W., Berk, A., Bernstein, L.S., Acharya, P.K., Miller, D. and Lewis, P. (2002) FLAASH, a MODTRAN4-based atmospheric correction algorithm, its application and validation. In Geoscience and Remote Sensing Symposium, 2002.IGARSS'02. 2002 IEEE Internat., v.3, pp.1414-1418).

Crosta, A.P., Sabine, C. and Taranik, J.V. (1998) Hydrothermal alteration mapping at Bodie, California, using AVIRIS hyperspectral data. Remote Sensing Environ., v.65(3), pp.309-319.

Crowley, J.K. (1993) Mapping playa evaporate minerals with AVIRIS data: A first report from Death Valley, California. Remote Sensing Environ., v.44(2-3), pp.337-356.

Deb, M., and Bhattacharya, A. K. (1980). Geological setting and conditions of metamorphism of Rajpura-Dariba polymetallic ore deposit, Rajasthan, India. *In:* Proceedings of the 5th IAGOD Symposium, Scheweizerbart'sche Verlagsbuchhandlung, Sttutgart, pp.679-697.

Farrand, W.H., (1997)Identification and mapping of ferric oxide and oxyhydroxide minerals in imaging spectrometer data of Summitville, Colorado, USA, and the surrounding San Juan Mountains. Internat. Jour. Remote Sensing, v.18(7), pp.1543-1552.

Fatima, K., Khattak, M.U.K., Kausar, A.B., Toqeer, M., Haider, N. and Rehman, A.U. (2017). Minerals identification and mapping using ASTER satellite image. Jour. Appld. Remote Sensing, v.11(4), 046006.

Felde, G.W., Anderson, G.P., Cooley, T.W., Matthew, M.W., adler – Golden, S.M., Berk, A., and Lee, J. (2003) Analysis of Hyperion data with the FLAASH atmospheric correction algorithm. In Geoscience and Remote Sensing Symposium, IGARSS'03 Proceedings. 2003 IEEE Internat., v.1, pp.90-92.

Gad, S. and Kusky, T. (2007) ASTER spectral ratioing for lithological mapping in the Arabian–Nubian shield, the Neoproterozoic Wadi Kid area, Sinai, Egypt. Gondwana Res., v.11(3), pp.326-335.

Gaffey, S.J. (1986) Spectral reflectance of carbonate minerals in the visible and near infrared (0.35-2.55 microns); calcite, aragonite, and dolomite. American Mineral., v.71(1-2), pp.151-162.

Goetz, A.F., Vane, G., Solomon, J.E. and Rock, B.N.(1985) Imaging spectrometry for earth remote sensing. Science, v.228(4704), pp.1147-1153.

Govil, H., Tripathi, M. K., Diwan, P., Guha, S., and Monika (2018) Identification of Iron Oxides Minerals In Western Jahajpur region, India using AVIRIS-NG hyperspectral remote sensing, Int. Arch. Photogramm. Remote Sens. Spatial Inf. Sci., XLII-5, 233-237, https://doi.org/10.5194/isprs-archives-XLII-5-233-2018.

Guha, A., Chakraborty, D., Ekka, A.B., Pramanik, K., Kumar, K.V., Chatterjee, S., Subramanium, S. and Rao, D.A. (2012) Spectroscopic study of rocks of Hutti-Maski schist belt, Karnataka. Jour. Geol. Soc. India, v.79(4), pp.335-344.

Guha, A., Vinod Kumar K., Porwal A., Rani K., Singaraju V., Singh R.P. (2018) Reflectance spectroscopy and ASTER based mapping of rock-phosphate in parts of Paleoproterozoic sequences of Aravalli Group of rocks, Rajasthan, India. Ore Geol. Rev., DOI: 10.1016/j.oregeorev.2018.02.021.

Guha, A., Kumar, K.V., Porwal, A., Rani, K., Sahoo, K.C., Kumar, S.A., Singaraju, V., Singh, R.P., Khandelwal, M.K., Raju, P.V. and Diwakar, P.G. (2019) Reflectance spectroscopy and ASTER based mapping of rock-phosphate in parts of Paleoproterozoic sequences of Aravalli Group of rocks, Rajasthan, India. Ore Geol. Rev., v.108, pp.73-87.

Green, A. A., Berman, M., Switzer, P. and Craig, M. D. (1988) A transformation for ordering multispectral data in terms of image quality with implications for noise removal: IEEE Trans. Geoscience and Remote Sensing, v.26(1), pp.65-74.

Gupta, S., Golani, P.R., Kirmani, I.R., and Chander, S. (2010) Tourmaline as metallogenic indicator: Examples from paleo-proterozoic Pb-Zn and Cu-Au deposits of Rajasthan. Jour. Geol. Soc. India, v.76(3), pp.215-243.

Jain, R. and Sharma, R.U. (2018) Mapping of Mineral Zones using the Spectral Feature Fitting Method in Jahazpur belt, Rajasthan, India. Internat. Res. Jour. Engg. Tech., (IRJET), v.5, pp.562-567.

Kalinowski, A. and Oliver, S. (2004) ASTER mineral index processing manual. Remote Sensing Applications, Geoscience Australia, v.37, pp.36.

Kratt, C., Calvin, W.M. and Coolbaugh, M.F.(2010)Mineral mapping in the Pyramid Lake basin: Hydrothermal alteration, chemical precipitates and geothermal energy potential. Remote Sensing Environ., 114(10), pp.2297-2304.

Kruse, F.A., Lefkoff, A.B. and Dietz, J.B. (1993) Expert system-based mineral mapping in northern Death Valley, California/Nevada, using the airborne visible/infrared imaging spectrometer (AVIRIS). Remote Sensing Environ., v.44(2-3), pp.309-336.

Kruse, F. A., Perry, S. L., and Caballero, A. (2002) Integrated multispectral and hyperspectral mineral mapping, Los Menucos, Rio Negro, Argentina, Part II: EO-1 Hyperion/AVIRIS comparisons and Landsat TM/ASTER extensions. *In:* Proc. 11th JPL Airborne Geoscience Workshop. Jet Propulsion Laboratory, Pasadena, California.

Kruse, F.A., Boardman, J.W. and Huntington, J.F. (2003) Comparison of airborne hyperspectral data and EO-1 Hyperion for mineral mapping. IEEE Trans. Geoscience and Remote Sensing, v.41(6), pp.1388-1400.

Kaufman, Y. J., Wald, A. E., Remer, L. A., Gao, B.-C., Li, R.-R., and Flynn, L. (1997) The MODIS 2.1-ìm Channel-Correlation with Visible Reflectance for Use in Remote Sensing of Aerosol. IEEE Trans. Geoscience and Remote Sensing. v.35, pp.1286-1298.

Lillesand, T., Kiefer, R.W. and Chipman, J. (2014) Remote sensing and image interpretation. John Wiley & Sons.

Matthew, M.W., Adler-Golden, S.M., Berk, A., Richtsmeier, S.C., Levine, R.Y., Bernstein, L.S., Acharya, P.K., Anderson, G.P., Felde, G.W., Hoke, M.L., Ratkowski, A.J., Burke, H. K., Kaiser R. D., Miller D.V., (2000, August). Status of atmospheric correction using a MODTRAN4-based algorithm. *In:* Algorithms for multispectral, hyperspectral, and ultraspectral imagery VI (Vol. 4049, pp.199-208).International Society for Optics and Photonics.

Milton, E.J., Schaepman, M.E., Anderson, K., Kneubühler, M. and Fox, N. (2009) Progress in field spectroscopy. Remote Sensing Environ., v.113, pp.S92-S109.

Mukherjee, A.D. (1988) Metallogeny and controls of mineralisation in Aravalli mountain belt. Mem. Geol. Soc. India, no.7, pp.351-362.

Mukherjee, R. and Venkatesh, A.S. (2017) Chemistry of magnetite-apatite from albitite and carbonate-hosted Bhukia Gold Deposit, Rajasthan, western India–An IOCG-IOA analogue from Paleoproterozoic Aravalli Supergroup: Evidence from petrographic, LA-ICP-MS and EPMA studies. Ore Geol. Rev., v.91, pp.509-529.

NASA, 2018,https://aviris-ng.jpl.nasa.gov/data.html

Price, J.C., 1995. Examples of high resolution visible to near-infrared reflectance spectra and a standardized collection for remote sensing studies. Remote Sensing, v.16(6), pp.993-1000.

Rani, K., Guha, A., Mondal, S., Pal, S.K., and Kumar, K.V. (2019) ASTER multispectral bands, ground magnetic data, ground spectroscopy and space-based EIGEN6C4 gravity data model for identifying potential zones for gold sulphide mineralization in Bhukia, Rajasthan, India. Jour. Appld. Geophys., v.160, pp.28-46.

Rowan, L.C. and Mars, J.C. (2003) Lithologic mapping in the Mountain Pass, California area using advanced spaceborne thermal emission and reflection radiometer (ASTER) data. Remote Sensing Environ., v.84(3), pp.350-366.

Roy, A.B. and Paliwal, B.S. (1981) Evolution of lower Proterozoic epicontinental deposits: Stromatolite-bearing Aravalli rocks of Udaipur, Rajasthan, India. Precambrian Res., v.14(1), pp.49-74.

Roy, A.B. and Jakhar, S.R., 2002. Geology of Rajasthan (Northwest India) precambrian to recent. Scientific Publishers.

Shaif, M., Siddiquie, F.N. and Mukhopadhyay, S. (2017) Petrographic Characteristics of Manganese Bearing Rocks of Banswara Manganese Ores Belt, District Banswara, Rajasthan (India). Open Jour. Geol., v.7(07), pp.1047.

Story, M. and Congalton, R.G. (1986) Accuracy assessment: a user's perspective. Photogrammetric Engg. Remote Sensing, v.52(3), pp.397-399.

Thorpe, A.K., Frankenberg, C., Aubrey, A.D., Roberts, D.A., Nottrott, A.A., Rahn, T.A., Sauer, J.A., Dubey, M.K., Costigan, K.R., Arata, C., and Steffke, A.M.,Hills, S., Haselwimmer, C., Charlesworth, D., Funk, C.C., Green, R.O., Lundeen S.R., Boardman, J.W., Eastwood, M.L., Sarture, C.M., Nolte, S.H., Mccubbin, I.B., Thompson, D.R. and McFadden, J.P. (2016) Mapping methane concentrations from a controlled release experiment using the next generation airborne visible/infrared imaging spectrometer (AVIRIS-NG). Remote Sensing Environ., v.179, pp.104-115.

Yamaguchi, Y. and Naito, C. (2003) Spectral indices for lithologic discrimination and mapping by using the ASTER SWIR bands. Internat. Jour. Remote Sensing, v.24(22), pp.4311-4323.

Van der Meer, F.D., Van der Werff, H.M., Van Ruitenbeek, F.J., Hecker, C.A., Bakker, W.H., Noomen, M.F., Van Der Meijde, M., Carranza, E.J.M., De Smeth, J.B. and Woldai, T. (2012) Multi-and hyperspectral geologic remote sensing: A review. Internat. Jour. Appld. Earth Observation and Geoinformation, v.14(1), pp.112-128.

(Received: 21 December 2018; Revised form accepted: 21 October 2019)